ITER Divertor Plasma Modelling with Consistent Core-Edge Parameters

A. S. Kukushkin 1), H. D. Pacher 2), G. W. Pacher 3), G. Janeschitz 4), D. Coster 5), A. Loarte 6), D. Reiter 7)

1) ITER IT, Boltzmannstr. 2, 85748 Garching, Germany; 2) INRS-EMT, Varennes, Québec, Canada; 3) Hydro-Québec, Varennes, Québec, Canada; 4) FZK-PL-Fusion, Karlsruhe, Germany; 5) Max-Planck Institut für Plasmaphysik, Garching, Germany; 6) EFDA, Garching, Germany; 7) FZ Jülich, Jülich, Germany

e-mail contact of main author: kukusha@itereu.de

Abstract. Results of a detailed study of the parameter space of the ITER divertor with the B2-Eirene code are presented. Relations between plasma parameters at the separatrix, the interface between the core and edge plasma, are parameterised to provide a set of boundary conditions for the core models. The reference ITER divertor geometry is compared once more with the straight target option and the possibility of controlling the edge density by shifting the plasma equilibrium in ITER is explored.

1. Introduction

Recent studies [1–4] have shown that there is an operational window for which the ITER divertor is expected to provide both acceptable target loading and the required efficiency of helium ash removal. The present paper is devoted to a further exploration of the parameter space of the ITER divertor with major emphasis on the consistency of the divertor operational window with the required core plasma performance. The rationale for these studies is the following.

The upstream plasma density saturates with an increase of the fuelling rate [3, 4], thus limiting the operational window to rather low plasma density at the separatrix, $n_s \sim$ (3 to 4)$\cdot 10^{19}$m^{-3}, which is consistent with experimental indications that good plasma confinement in the H-mode requires low separatrix density [5]. To produce sufficient fusion power and Q, the average plasma density in ITER must be 8-10$\cdot 10^{19}$m^{-3} with a flat density profile in the centre. Consequently, a significant density gradient must be sustained in the "pedestal" region just inside the separatrix, and thus considerable particle fluxes must traverse this region [3, 6]. Since the neutral particle influx across the separatrix also saturates at a comparatively low level [3, 4], an additional fuelling scheme such as pellet injection has to be employed. This results in a core fuelling rate comparable to, or higher than, the gas puffing rate [7], whereas most of the calculations [1–4] have been done for conditions of predominant gas fuelling. A difference in the mechanisms of energy transport by electrons and ions in the plasma core leads to unequal power transferred by these plasma components across the separatrix, P_e and P_i, [7] whereas $P_i = P_e$ had been assumed in [1–4]. Furthermore, if the saturation of the upstream density were caused by the V-shaped target of ITER, then moving the separatrix strike point upward would allow to increase n_s, adding to the operational flexibility of the machine.

2. Effect of partition of power input and fuelling

Consistency of the edge plasma parameters with the core can be ensured if one solves the equations for the edge plasma and for the core plasma simultaneously, matching the densities, temperatures, and fluxes at the separatrix. Given the different time scales and models for the core (hundreds of seconds, close to 1D) and edge (tens milliseconds, 2D), it is presently impractical to couple the codes directly. Instead, the solutions for the edge are parameterised in terms of the variables resulting from core simulations, and the output quantities from the 2D simulations are used as boundary conditions for the 1-1/2D core plasma code. The natural

choice for the edge input parameters is the input power to the SOL P_{SOL}, the pumping speed S_{DT}, the DT particle throughput Γ_{DT}, the fraction of the throughput supplied by core fuelling $\eta_c = \Gamma_{core}/\Gamma_{DT}$, the ratio of power input in the electron and ion channels $\xi_{ei} = P_e/P_i$, and the helium ion flux across the separatrix which is determined by the fusion power and the helium atom influx into the core. The output quantities, which serve as the boundary conditions for the core plasma, are the separatrix-averaged values of the electron and ion temperatures T_{e_sep} and T_{i_sep}, of electron, He, and C densities, n_{sep}, n_{He_sep} and n_{C_sep}, of DT and He neutral outfluxes from the divertor $\Gamma_{DT\_n\_sep}$ and $\Gamma_{He\_n\_sep}$, and of the mean energy of these neutrals E_{DT_sep} and E_{He_sep}. Besides this, the peak power loading of the target q_{pk} is used to constrain the operational window of the core plasma. A first parametrisation of this kind was presented in [4] where the cases considered were mostly gas-fuelled and had $\xi_{ei} = 1$. It was shown that a two-regime power law scaling could be constructed, which fitted the output data quite well. The point where the density started to saturate for gas puffed cases (and near which the inner divertor detached) was found to delimit the two regimes of divertor operation having different exponents in the power law scalings. The input parameter space was essentially three-dimensional: no data was yet available for the ξ_{ei} variation and only a few points were available for core-fuelled cases (η_c variation). Taking these variations into account increases the dimensionality of the input parameter space from three to five, which makes full coverage of the parameter space in 2D calculations rather problematic. Therefore, we will concentrate here on the effect of these two new variables, having fixed $P_{SOL} = 100$ MW and $S_{DT} = 20$ m^3/s for the newer simulations and use the scalings obtained in [4] to parameterise the solution in P_{SOL} and S_{DT}.

For this study, we have six series of runs: three values of $\xi_{ei} = 1/3$, 1, and 3, and two fuelling scenarios: full core fuelling without gas puff ($\eta_c = 1$) and low core fuelling ($\eta_c = 0.3$ to 0.06). Fig. 1a shows the variation of q_{pk} with the neutral pressure in the private flux region (PFR) $p_{DT} = \Gamma_{DT}/ S_{DT}$. All the data points lie on the same curve, i.e. neither ξ_{ei} nor η_c affects q_{pk}, and therefore the scaling for q_{pk} remains the same as in [4]. This is plausible, since energy equipartition in the divertor region is fast, and the particle flows are dominated by recycling fluxes which are much stronger than the throughput, so that the behaviour of the divertor plasma is insensitive to the detail of energy and particle input to the edge. Note that this is not trivial, since the peak power load is composed of power resulting from conduction, convection, recombination and radiation.

However, the interface parameters, such as upstream densities and temperatures or neutral influxes, depend on the plasma parameters in the SOL which depend on ξ_{ei} and η_c. In Fig. 1b, the separatrix-average electron density n_{sep} is plotted as a function of p_{DT} for different values of ξ_{ei} and η_c. No n_{sep} saturation is seen for $\eta_c = 1$, although at the highest density for $\xi_{ei} = 1$, plasma in the inner divertor is already fully detached. There are two mechanisms which could explain the continued rise of n_{sep} by the core fuelling. First, particles entering the SOL from the core must be transported along and across the magnetic field, and this leads to an increase of n_s along with an increase of the flux (the ratio of $n_{sep}/n_s \approx 1.14$ is approximately constant). In the gas-puffed case, the particles are mostly deposited in the outer part of the SOL and the density gradients in the separatrix region are smaller. Second, an increase of the particle flux along the separatrix enhances the convective transport of energy, therefore reducing the conductive components. This results in a reduction of the upstream plasma temperature with corresponding increase – because of the pressure balance along the field – of n_s. Furthermore, a reduction of n_{sep} when ξ_{ei} decreases, Fig. 1b, can be attributed to the different electron and ion heat conductivities. Indeed, an increase of the ion heat flux should cause an increase of the ion temperature upstream which leads to a preferential increase of the conductive component of the flux due to the strong non-linear temperature dependence of the parallel heat

conductivity, and the electron temperature changes in the opposite direction. The increase of the ion temperature is stronger than the reduction of the electron temperature because of the lower ion heat conductivity, so that lower n_s is required to satisfy the pressure balance.

Following the approach of [4], we introduce the fuelling factor $f_{fuel} = 1 + 0.18\eta_c$ and the factor $f_{He} = 0.21\left(5Q/(Q+5)\right)\left(1-f_{rad}\right)^{-1}$ which relates the helium particle source to the input power P_{SOL}. We distinguish two regimes with different values of exponents in the fitting expressions, and we restrict our approximation to the lower density regime for which n_{sep} shows no sign of saturation [5]. The exponents in the fitting expressions for the plasma parameters at the critical point where the two regimes meet are given in the Table 1, and for the plasma parameters for a working point in the non-saturated regime in Table 2. For example, at the critical point, $q_{pk\_\#} = f_{fuel}^{\ -1.7} P_{\#}^{\ 1.26}$ where $q_{pk\_\#}$ is q_{pk} in units of 7.55 MW/m^2 and $P_{\#}$ is P_{SOL} in units of 100 MW. In Fig. 2, n_{sep} and n_{He_sep} are plotted according to the power law fit of Table 2; the fit is seen to be quite good.

TABLE 1. EXPONENTS IN THE PARAMETER SCALING AT THE CRITICAL POINT

	scale	q_{pk}	n_{sep}	$\Gamma_{DT\_n\_sep}$	n_{He_sep}	$\Gamma_{He\_n\_sep}$	T_{e_sep}	T_{i_sep}	Γ_{DT}
scale		7.55 MW/m^2	$3.89\cdot10^{19}$ m^{-3}	16.4 Pa·m^3/s	$3.06\cdot10^{17}$ m^{-3}	0.512 Pa·m^3/s	162 eV	270 eV	124 Pa·m^3/s
f_{He}	1	-	-	-	+1	+1	-	-	-
f_{fuel}	1	–1.7	+1.25	–2.5	–5	–5.42	–0.4	–0.9	+2
S_{DT}	20 m^3/s	-	-	+0.3	–1	–1	–0.02	–0.04	+1
P_{SOL}	100 MW	+1.26	+0.55	-	+0.7	0.52	+0.32	+0.36	+0.87
ξ_{ei}	1	-	+0.05	-	–0.1	-	+0.049	–0.115	-

TABLE 2. EXPONENTS IN THE PARAMETER SCALING IN TERMS OF DIVERTOR PRESSURE Γ_{DT}/S_{DT} FOR THE NON-SATURATED REGIME (THROUGHPUT BELOW CRITICAL)

	scale	q_{pk}	n_{sep}	$\Gamma_{DT\_n\_sep}$	n_{He_sep}	$\Gamma_{He\_n\_sep}$	T_{e_sep}	T_{i_sep}
scale		7.55 MW/m^2	$3.89\cdot10^{19}$ m^{-3}	16.4 Pa·m^3/s	$3.06\cdot10^{17}$ m^{-3}	0.512 Pa·m^3/s	162 eV	270 eV
f_{He}	1	-	-	-	+1	+1	-	-
f_{fuel}	1	-	+0.53	–3	–1	–1	–0.06	–0.32
S_{DT}	20 m^3/s	-	-	+0.3	–1	–1	–0.02	–0.04
P_{SOL}	100 MW	+2	+0.24	–0.22	+2.44	+2.44	+0.47	+0.61
ξ_{ei}	1	-	+0.05	-	–0.1	-	+0.05	–0.116
Γ_{DT}/S_{DT}	6.2 Pa	–0.85	+0.36	+0.25	–2	–2.21	–0.17	–0.29

3. Effect of moving the strike-point position

In order to check whether the limitation of the upstream density is determined by the V-shaped target, several density scans via gas puff have been done. The variation of the divertor geometry includes the straight target as in [2] but with the same finite transparency of the liners in PFR as for the standard model [4], and a variation of the x-point position for the standard V-shaped targets shown in Fig. 3. The results, Fig. 4, indicate that the reference ITER divertor geometry, although optimised for low n_s, does not significantly restrict the achievable n_s. Indeed, a similar n_s saturation is seen for the straight target geometry at a level ~ 8% higher than for the V-shaped target. A moderate upward shift of the strike-point position brings approximately the same gain in n_s, although at somewhat higher q_{pk}.

However, further displacement of the strike points leads to the appearance of a bifurcation in

the state of the divertor plasma (Δ = 12 cm in Fig. 4). This bifurcation looks similar to a physics picture developed in a simple model including only one divertor [8], which demonstrated that two states of the divertor plasma corresponding to the same total amount of particles in the SOL and divertor plasma N_{SOL} can exist. These states differ by the distribution of the particles along the SOL and divertor: the particles can be more concentrated in the divertor or more distributed in the SOL (n_s is still much lower than the divertor density). At the transition between these states, the neutral pressure in the divertor is expected to vary significantly, as is verified for the present simulation in Fig. 5, which shows the calculated p_{DT} plotted against N_{SOL}. Because N_{SOL} varies slowly, the transition between the two stable branches can occur only along approximately vertical lines. A stepwise change of neutral pressure in the divertor and considerable excursions of the divertor plasma parameters are expected at the transition. In particular, the q_{pk} values can vary by a factor 2 (compare Fig. 4 and Fig. 5). The only point we have for Δ = 24 cm (Fig. 4) belongs apparently to the high-pressure branch, and this is an indication of the variation of plasma parameters at bifurcation becoming stronger as the separatrix strike point moves away from the pumping duct. The bifurcation does not occur over the nominal operating range which was used for all the other results presented. Note that it is undesirable from a control point of view to operate in the region of parameter space where such a bifurcation occurs, since there small variations of the control quantity (throughput) can lead to large excursions of the parameters.

4. Conclusions

The extensive modelling effort reported in the present paper has led to an efficient power law parametrisation of the plasma and neutral parameters at the interface between the edge and core plasma, making it finally possible to model the ITER core plasma performance in a way consistent with the divertor parameters [7].

The V-shaped target geometry employed in ITER does not impose additional constraints on the operational flexibility in terms of the achievable separatrix density.

A variation of the x-point position offers some control over the achievable separatrix density. However, bifurcation of the divertor plasma parameters can limit the utility of this control method. More work is needed to elucidate the exact nature of this bifurcation, to optimise the divertor geometry, and to extend the scaling to cases having re-eroded carbon at the walls and/or additional impurity seeding.

References

[1] KUKUSHKIN, A.S., et al., J. Nucl. Mater. **290–293** (2001) 887.
[2] KUKUSHKIN, A.S., et al., Nucl. Fusion **42** (2002) 187.
[3] KUKUSHKIN, A.S., PACHER, H.D., Plasma Phys. Control. Fusion **44** (2002) 931
[4] PACHER, H.D., et al., "Scaling of ITER Divertor Parameters - Interpolation from 2D Modelling and Extrapolation", 15th PSI Conference, Gifu, 2002; to be published in J. Nuclear Mater. 2003.
[5] ITER Physics Basis. Nucl. Fusion **39** (1999) 2137.
[6] PACHER, G.W., et al., 28th EPS Conference on Contr. Fusion and Plasma Phys. Funchal, 18-22 June 2001, ECA Vol. 25A (2001) 625
[7] PACHER, G.W., et al., "ITER Plasma-SOL Interface parameters from 1-D predictive Model for Energy and Particle Transport", this conference
[8] KRASHENINNIKOV, S.I., KUKUSHKIN, A.S., Sov. Tech. Phys. Lett. **14** (1988) 228

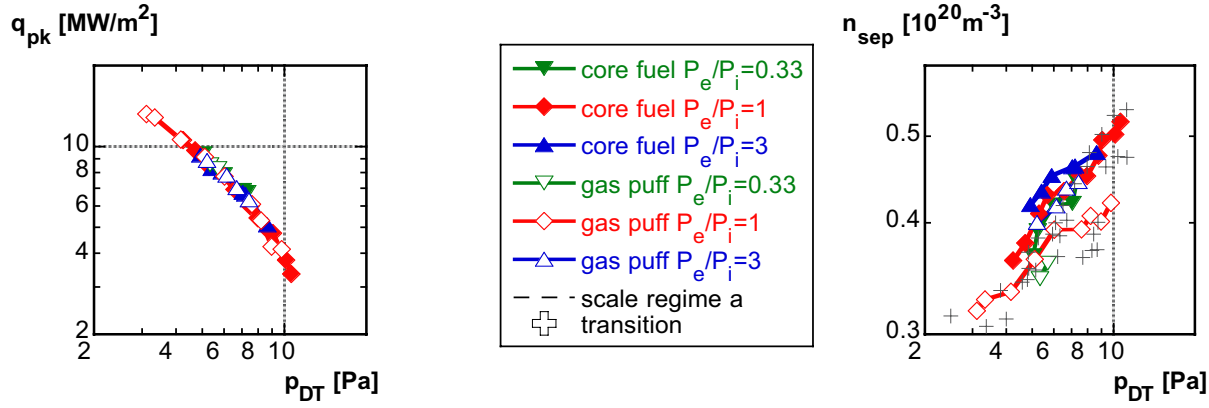

(a) (b)

FIG. 1. (a) Peak power load on the target q_{pk} vs. neutral pressure in PFR $p_{DT} = \Gamma_{DT}/S_{DT}$ for different fuelling scenarios and different values of the electron-to-ion power input ratio. (b) Separatrix-average density n_{sep} vs. p_{DT} for different fuelling scenarios and different values of the electron-to-ion power input ratio. The data from [4] are shown with crosses.

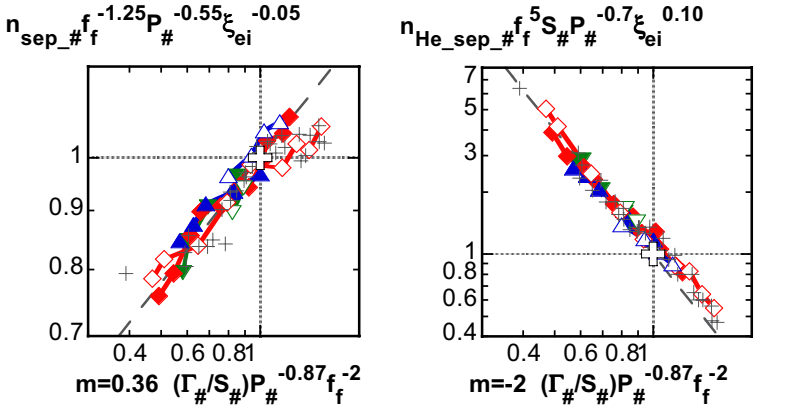

FIG. 2. Fit to the separatrix-average densities n_{sep} (left) and n_{He_sep} (right), which is used as the boundary condition for the core model [7]. The legend is the same as for Fig. 1. The subscript "#" means normalisation to the constants of Tables 1 and 2.

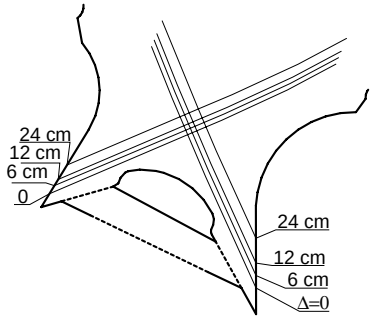

FIG. 3. Variation of the x-point position used for the explorations. The position of the strike points are marked with corresponding displacement of the x-point.

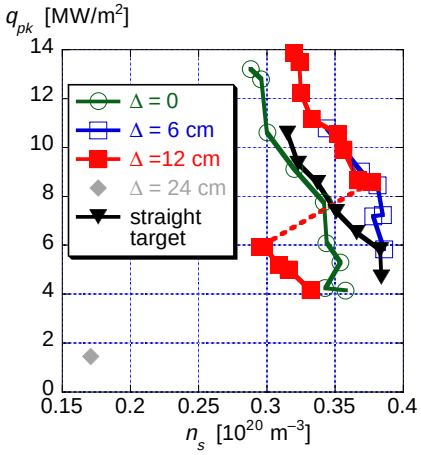

FIG. 4. Peak power loading on the target vs. upstream plasma density for different values of the x-point displacement Δ. The results for the straight target are also shown here. The curve for Δ = 12 cm reveals a bifurcation: no stable points are found on the dashed part of the curve.

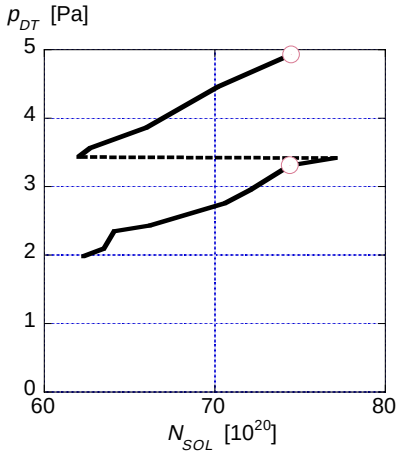

FIG. 5. Neutral pressure in the PFR vs. the total number of electrons in the edge plasma for Δ = 12 cm. The range where $p_{DT}(N_{SOL})$ is multi-valued indicates the bifurcation.